

Paul F. Prososki\*

Texas Tech University, Lubbock, Texas

Christopher C. Weiss

Texas Tech University, Lubbock, Texas

## 1. INTRODUCTION

Though it has been long known that the drylines are associated with cumulus clouds and thunderstorms, forecasting convective initiation (CI) has proven difficult along this type of boundary (Owen 1966; Ziegler and Rasmussen 1998). Recent studies, particularly from the 2002 International H<sub>2</sub>O Project (IHOP), show that vertical vorticity maxima, or misocyclones, exist in boundaries such as cold fronts and drylines (e.g., Arnott et al. 2006; Marquis et al. 2007). Misocyclones have been simulated numerically along such fronts (Buban et al. 2012), and have been proposed to be, at least in part, responsible for clouds and CI along such boundaries (Arnott et al. 2006). Studies have also suggested that the intersection of fronts and horizontal vorticity in the form of horizontal convective rolls (HCRs) may produce locally enhanced upward vertical motion and have been shown to be associated with clouds (Wilson et al. 1992; Atkins et al. 1995; Atkins et al. 1998), and are theorized to produce dryline misocyclones (Buban et al. 2007).

To test that HCR-dryline intersections can produce misocyclones and that horizontal shear is necessary for the existence of dryline misocyclones, the field campaign in spring 2012 made use of two Texas Tech Ka band (TTUKa) radars to observe the dryline and its misocyclones. To maximize data resolution and observe the lowest levels of the misocyclones, small baselines of 4-7 km were used with the lowest possible elevation angles.

## 2. ANALYSIS METHODOLOGY

SOLOii, DREADER, and hand editing were used to quality control and clean radar data. Then, a two-pass Barnes analysis was used to objectively analyze data to a regular 40 m grid, in

accordance with Koch et al. (1983), including data with a crossing angle between 25° and 155°. A smoothing parameter of  $\kappa=0.018 \text{ km}^2$  and convergence parameter of  $\gamma=0.4$  were used for the analysis, as suggested by Pauley and Wu (1990).

When available, satellite data are obtained to compare observed clouds to dryline structure and vorticity fields. In such cases, data are compared to radar analyses by converting the latitude and longitude to a distance using a flat-earth projection. Error from this method is insignificant due to the low resolution of the satellite features compared to the small domain size of radar analyses.

To assess the dependence of vorticity on horizontal shear, the wind component in the along-boundary direction was calculated from the dual-Doppler analyses to determine if instability criteria are met. For example, a Rayleigh instability for horizontal shear should exist when there is an inflection point in the along-boundary wind profile. That is,

$$\frac{d^2v}{dx^2} = 0 \quad (1)$$

where  $v$  is the along-boundary wind component and  $x$  is distance in the cross-boundary direction. Furthermore, Fjortoft gives a more stringent criterion for instability to exist:

$$(v - v_i) \frac{d^2v}{dx^2} < 0 \quad (2)$$

where  $v_i$  is the boundary-parallel wind at the inflection point (Fig. 1).

## 3. 30 APRIL 2012 CASE – LEVELLAND, TX

### Overview

On 30 April 2012, two TTUKa radars intercepted an early developing dryline, which was had already begun to sharpen into a fineline on the LBB WSR-88D by 1830 UTC (Fig. 2). By 1925 UTC the two TTUKa radars were deployed and began collecting data just south and west of

---

\* Corresponding author address: Paul F. Prososki, Texas Tech University, Atmospheric Science Group, Department of Geosciences, Lubbock, TX, 79409; e-mail: [paul.prososki@huskers.unl.edu](mailto:paul.prososki@huskers.unl.edu)

Levelland, TX. At 2035 UTC observations ceased as the moderate CAPE ( $\sim 1600 \text{ J kg}^{-1}$ ) and high CIN ( $\sim 200 \text{ J kg}^{-1}$ ) environment produced supercells both about 100 km north and south of the observation domain. Visible satellite imagery shows a thin line of cumulus clouds along the dryline about three minutes after the deployment began (Fig. 3). Field crews observed clouds increasing in size and number during the course of the deployment.

The dryline progressed from a northwest-southeast orientation to nearly a west-northeast orientation over the course of observation. Power returned to the radar was considerably greater on the moist-air side of the dryline throughout the period of observation, perhaps due to a shallower boundary layer increasing the density of scatterers. At times, power returned on the dry air side was insufficient for dual-Doppler analysis.

Reflectivity structures were clearly present and continually evolving in the dry air, beginning as regular linear features, morphing into regular hexagonal cellular forms, and reverting back into more linear shapes. At times, the linear horizontal structures (LHSs) even crossed each other. Due to insufficient data, it is impossible to determine the nature of such structures, including whether or not the LHSs are at times HCRs.

Dry air structures commonly intersected the dryline, and the dryline was observed to inflect significantly before collapsing back into a less complex, thinner and straighter boundary form. Frequently, the evolution of the dryline into complex forms was associated with the presence of misocyclones and LHS intersections.

### *Results*

Dual-Doppler analyses show that at times misocyclones remain anchored directly on the intersection of an LHS and the dryline. At other times there is no misocyclone anchored to an LHS-dryline intersection. One novel observation is that of the amplification of vorticity along the LHS-dryline intersection point. At 1948 UTC, a misocyclone propagated up the dryline, through an LHS-dryline intersection, and approximately doubled its vorticity. It retained its increased vorticity until reaching the edge of the domain ten minutes later.

Another unique observation not well documented in previous studies is the existence of misocyclones off the mesoscale boundary. That is, misocyclones were observed to propagate along dry air LHSs towards the dryline, make a left turn onto the dryline, then to continue propagating

up the dryline similarly to the motion of any other dryline misocyclone.

At times when the dryline itself appeared to spin and fold over itself, misocyclones were observed to pass each other, sometimes with one or more misocyclones actually moving against the normal direction of misocyclone propagation. It was also observed that the motion of two or more misocyclones resembled a Fujiwhara interaction, circulating around a central point. Larger singular misocyclones did appear to distort the dryline and LHSs, and convergence tended to be enhanced upstream and downstream of misocyclones within the boundary, similar to observations by Marquis et al. (2007).

Comparison of satellite and radar data showed one cloud over the moist air mass directly in line with a dry air LHS. Two other clouds appeared on the edge of the domain, each over the moist air directly south of prominent dryline vorticity features, or dryline spinups containing multiple misocyclones (Fig. 4).

## 4. CONCLUSIONS AND FUTURE WORK

The high resolution nature of this study has revealed previously unresolved phenomena that may provide clues to the origins of misocyclones, factors affecting their lifecycles, and effects of misocyclones on the larger environment, such as cloud formation. Key findings include:

- Misocyclones existing off the mesoscale boundary, propagating along LHSs, and continuing up the dryline.
- Amplification of existing dryline misocyclones at the intersection of LHSs with the dryline.

Also noteworthy results are the offset of convergence from the vorticity maxima and the association of clouds with observable features. While the limited domain size makes it difficult to draw conclusions with regards to the clouds, or even explain why one cloud was over the moist air while two others were above dry air, it is possible that the dry air cloud was older in its lifecycle and had more time to advect away from the mesoscale boundary.

Amplification of misocyclones at LHS-dryline intersections and the moist air cloud could suggest enhanced vertical velocity at these intersections. Enhanced vertical motion would both help air parcels reach the LCL and stretch pre-existing vertical vorticity. The anchoring of misocyclones to these intersections could also support the theory of tilting horizontal vortex lines

at the mesoscale boundary. The existence of misocyclones off the boundary, however, suggests that this theory alone is likely insufficient to fully explain misocyclogenesis. These LHS misocyclones could conversely be the result of shear instabilities.

Future research will focus on horizontal instabilities, though a proof of concept has been provided in Figure 5. The degree of Fjortoft instability can be compared to the amplification of vorticity. Future work may also compare the atmospheric boundary layer (ABL) depth from range-height indicators (RHIs) transecting the dryline. Relating ABL depths with LHS spacing may provide clues to the nature of the reflectivity structures, including whether or not they could at times be HCRs.

## 5. ACKNOWLEDGEMENTS

The authors would like to thank Anthony Reinhart, Patrick Skinner, and Scott Gunter, as well as other students, of Texas Tech University for their time given to field work. Gratitude is also offered for discussions with Conrad Ziegler of the National Severe Storms Laboratory and Adam Houston of the University of Nebraska.

## 6. REFERENCES

- Arnott, Nettie R., Yvette P. Richardson, Joshua M. Wurman, Erik M. Rasmussen, 2006: Relationship between a Weakening Cold Front, Misocyclones, and Cloud Development on 10 June 2002 during IHOP. *Mon. Wea. Rev.*, **134**, 311–335.
- Atkins, Nolan T., Roger M. Wakimoto, Conrad L. Ziegler, 1998: Observations of the Finescale Structure of a Dryline during VORTEX 95. *Mon. Wea. Rev.*, **126**, 525–550.
- , Roger M. Wakimoto, Tammy M. Weckwerth, 1995: Observations of the Sea-Breeze Front during CaPE. Part II: Dual-Doppler and Aircraft Analysis. *Mon. Wea. Rev.*, **123**, 944–969.
- Buban, Michael S., Conrad L. Ziegler, Edward R. Mansell, Yvette P. Richardson, 2012: Simulation of Dryline Misovortex Dynamics and Cumulus Formation. *Mon. Wea. Rev.*, **140**, 3525–3551.
- , Conrad L. Ziegler, Erik N. Rasmussen, Yvette P. Richardson, 2007: The Dryline on 22 May 2002 during IHOP: Ground-Radar and In Situ Data Analyses of the Dryline and Boundary Layer Evolution. *Mon. Wea. Rev.*, **135**, 2473–2505.
- Koch, Steven E., Mary desJardins, Paul J. Kocin, 1983: An Interactive Barnes Objective Map Analysis Scheme for Use with Satellite and Conventional Data. *J. Climate Appl. Meteor.*, **22**, 1487–1503.
- Marquis, James N., Yvette P. Richardson, Joshua M. Wurman, 2007: Kinematic Observations of Misocyclones along Boundaries during IHOP. *Mon. Wea. Rev.*, **135**, 1749–1768.
- Owen, J., 1966: A Study of Thunderstorm Formation Along Dry Lines. *J. Appl. Meteor.*, **5**, 58–63.
- Pauley, P. M., and X. Wu, 1990: The theoretical, discrete, and actual response of the Barnes objective analysis scheme for one- and two-dimensional fields. *Mon. Wea. Rev.*, **118**, 1145–1164.
- Wilson, James W., G. Brant Foote, N. Andrew Crook, James C. Fankhauser, Charles G. Wade, John D. Tuttle, Cynthia K. Mueller, Steven K. Krueger, 1992: The Role of Boundary-Layer Convergence Zones and Horizontal Rolls in the Initiation of Thunderstorms: A Case Study. *Mon. Wea. Rev.*, **120**, 1785–1815.
- Ziegler, Conrad L., Erik N. Rasmussen, 1998: The Initiation of Moist Convection at the Dryline: Forecasting Issues from a Case Study Perspective. *Wea. Forecasting*, **13**, 1106–1131.

# Fjortoft Instability

$$(V - V_i) \frac{d^2V}{dx^2} < 0$$

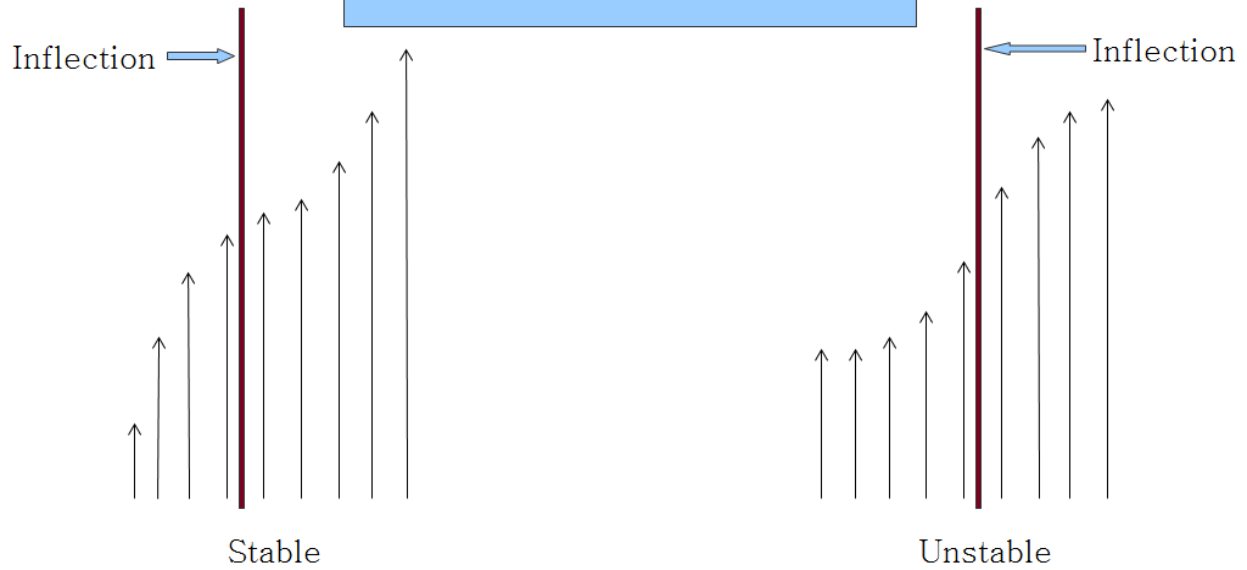
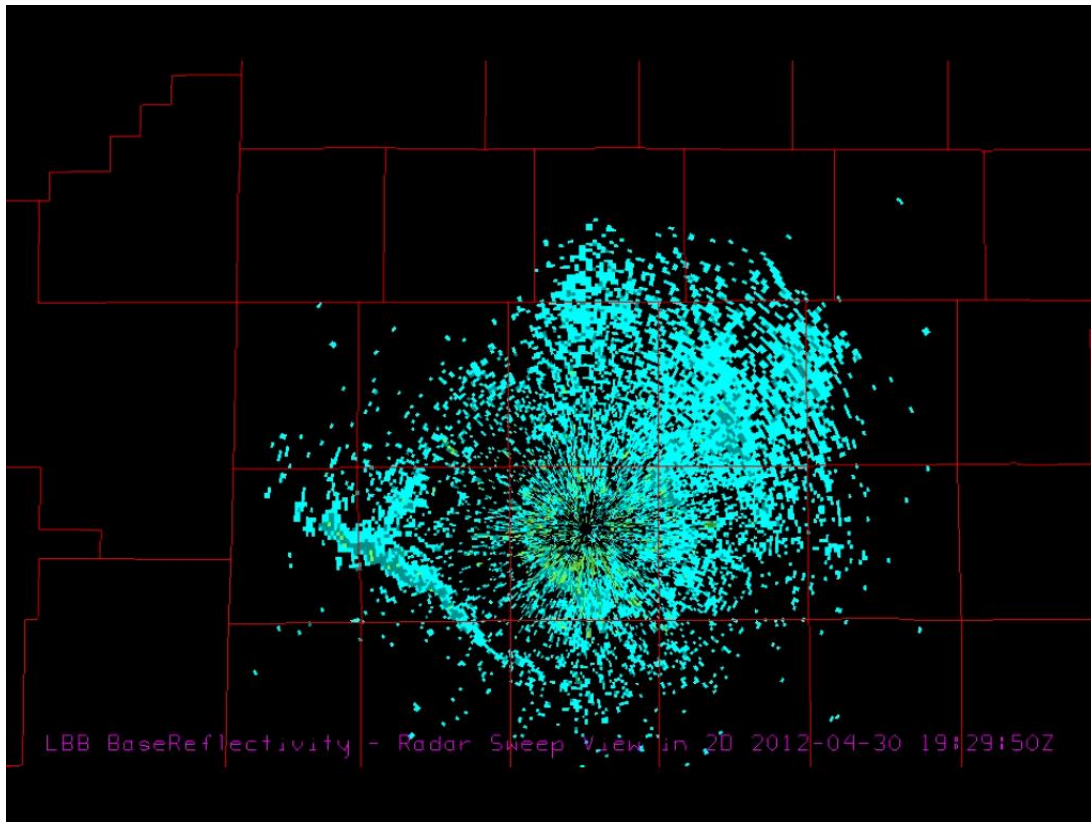


Figure 1 – Given the presence of an inflection within the shear zone, Fjortoft Instability exists when the side of the shear zone with less wind is concave up or the stronger wind side is concave down.



*Figure 2 – Weather Surveillance Radar 88 Doppler (WSR-88D) data from Lubbock, TX indicate the presence of a strong boundary – the dryline – across the western South Plains of West Texas. Deployment occurred in southwestern Hockley County, the county directly west of the country containing the WSR-88D.*

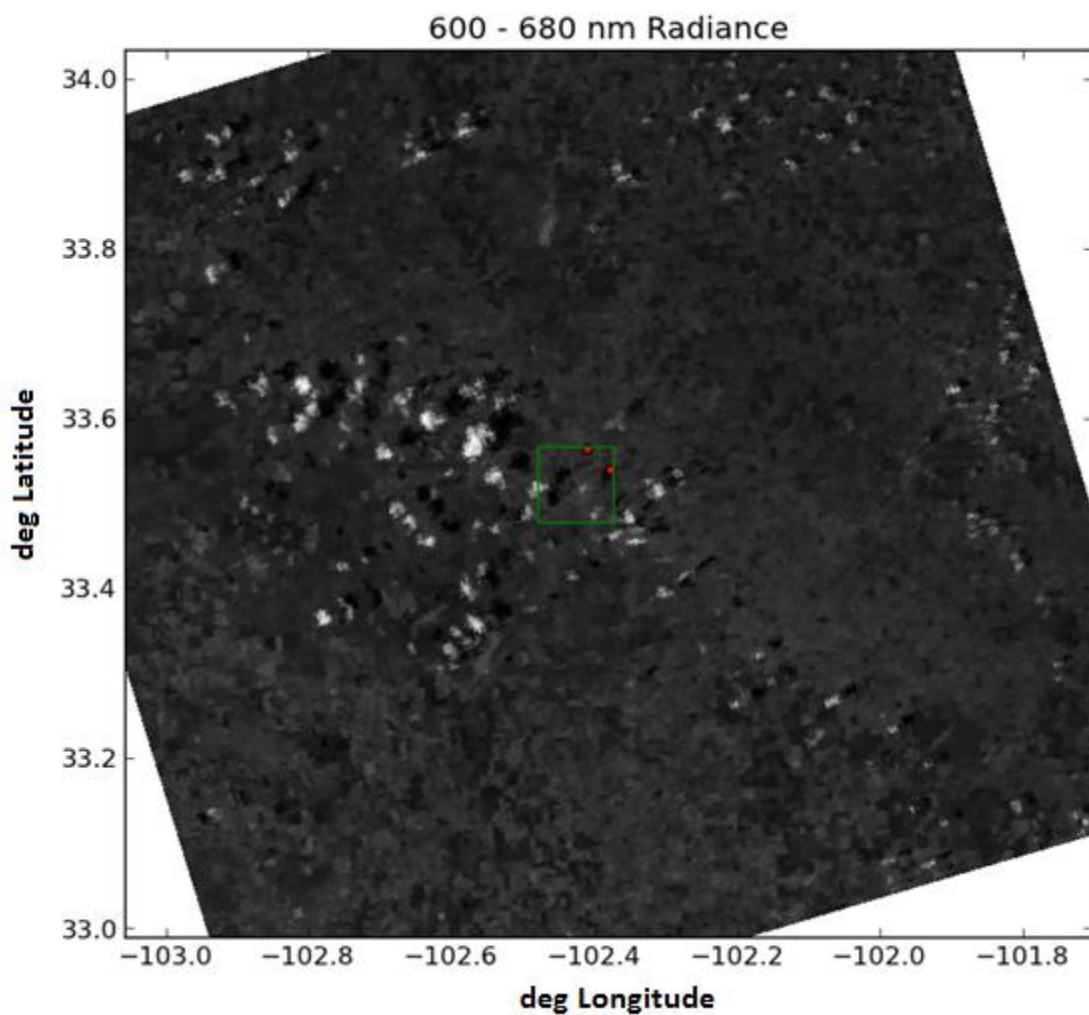


Figure 3 – 1928 UTC satellite image of West Texas from the 375 m resolution Visible Infrared Imaging Radiometer Suite (VIIRS) on the Suomi National Polar-orbiting Partnership (NPP) satellite. The green box indicates the 10x10 km observation domain, while the two red dots along the north and east edges indicate the position of the TTUKa radars, with a 4 km baseline. The line of clouds parallels the fineline in Figure 2.

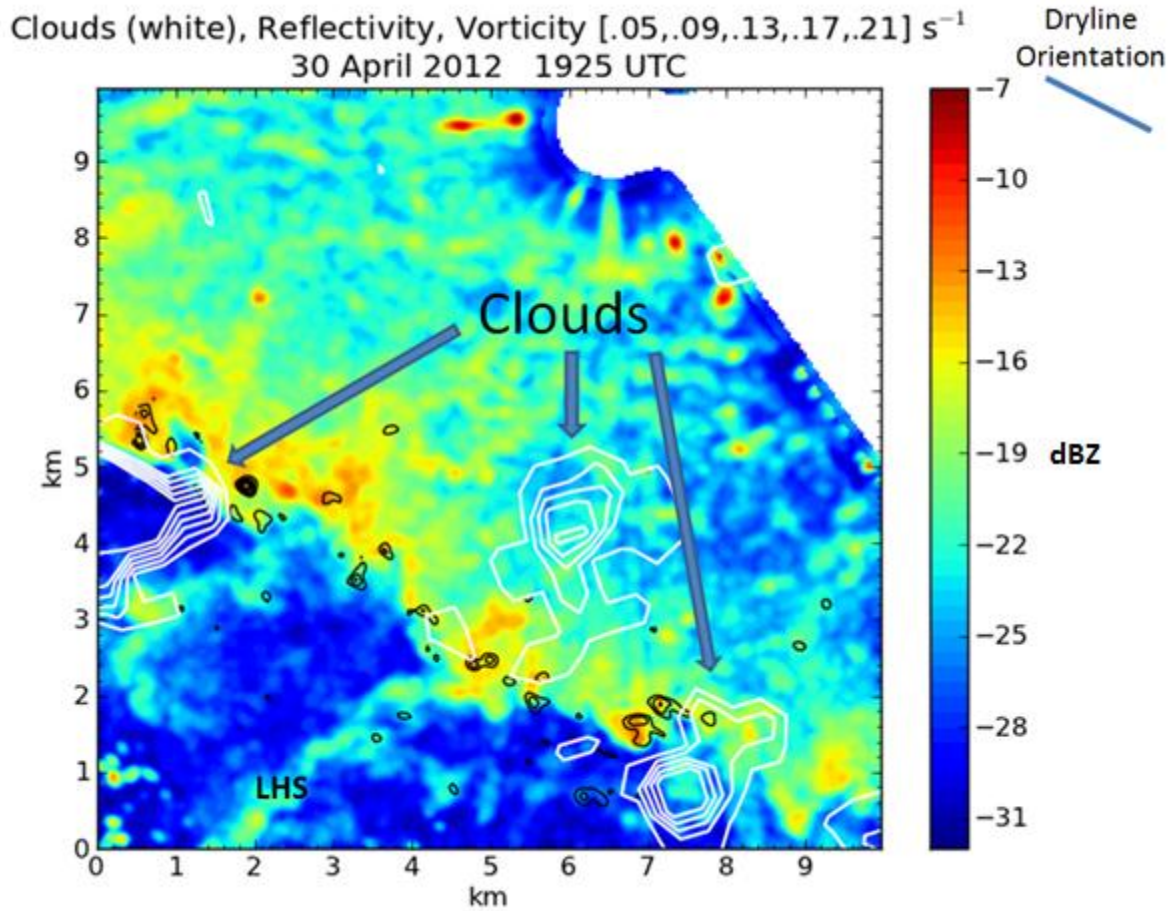


Figure 4 – Satellite cloud data (1928 UTC) overlaid on radar data (1925 UTC). The dryline is again oriented northwest to southeast with the moist air mass to the northeast where higher reflectivity exists. Within the dry air, two LHSs are visible extending into the dryline, one of which has a cloud aligned with it beyond the dryline. The other two clouds are located nearly above the dryline but directly south of distorted regions of the dryline containing misocyclones.

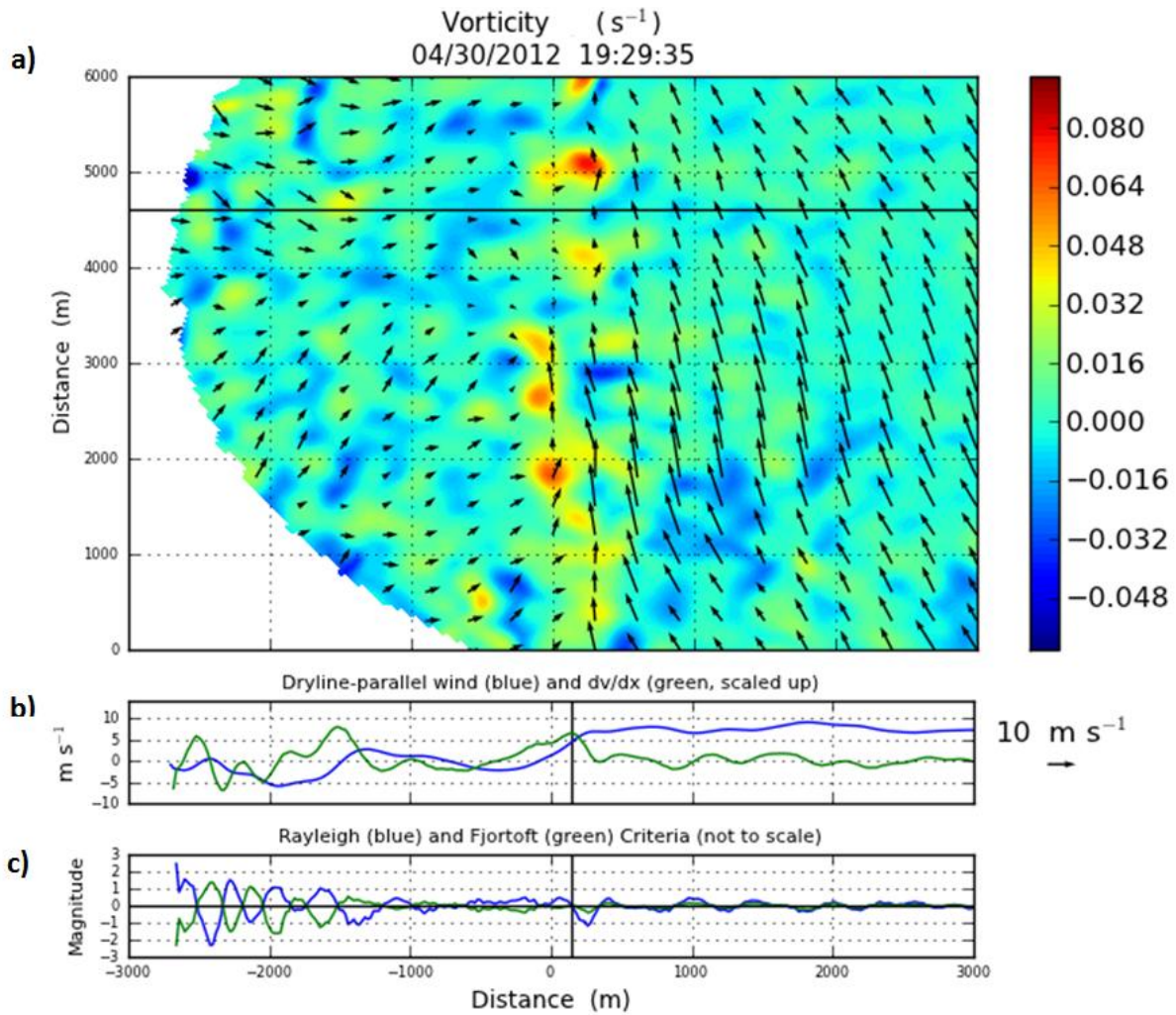


Figure 5– a) Radar data (vorticity) rotated such that the dryline is oriented north-south with a horizontal line shown to indicate the position of dryline transect data. b) The vertical wind component at this transect is then graphed, as is its derivative (Rayleigh criteria met when blue line = 0), and Fjortoft criteria (met when green line < 0). The vertical line represents the location of the inflection point used in the analysis. Note the low levels Fjortoft instability at the dryline at this point. During the few minutes following this snapshot, there is neither development of new misocyclones nor amplification of existing misocyclones in this region of the dryline.